ISABE 99-7283

Three-Dimensional Unsteady Turbomachinery Flow Analysis

S. H. Chen (Associate Professor), and L. C. Lee (Research Assistant)
Institute of Aeronautics and Astronautics,
National Cheng Kung University,
Tainan, Taiwan, Republic of China

ABSTRACT

A Loosely Couple Blade Row (LCBR) numerical method is developed to analyze the unsteady flow field of a three-dimensional multi-blade-row turbomachinery problem. This method allows the use of initial blade numbers for unsteady calculation and only one blade channel per blade row is used. Circumferential average approach to obtain a converged steady solution as the initial condition is adopted for unsteady calculation. Relatively, it not only maintains the blade configuration, but is also computationally more efficient. The numerical method used is a compressible viscous finite volume algorithm solving Reynolds averaged Navier-Stokes equations. Artificial dissipation terms similar to that used by Jameson is adopted to suppress the numerical oscillations. Four-Stage Runge-Kutta scheme is used to advance the flow equations in time. Residual smoothing and multi-grid techniques are employed to accelerate the convergence. Baldwin and Lomax algebraic turbulent model is used for the calculation of eddy viscosity. The UTRC (United Technologies Research Center) large scale turbine is used here as the test case. The unsteady flow predicted correlates well with data. The results indicate that the unsteady turbomachinery flowfield can be solved with single flow channel of unequal pitch on each blade row .

1. INTRODUCTION

Multistage turbomachinery calculations have becoming popular since mid 80's. The two main streams are circumferential average calculations and unsteady calculations. Among the circumferential average methods, representatives studies are from Ni [1989], Adamczyk [1990], Denton [1992] and Dawes [1992]. These methods have been used to replace the traditional row-by-row design methods used in industry for many years. However, these type of methods generally ignore the unsteady interactions between blade rows. Despite this kind of method ignores true unsteady interaction effects between blade rows, it allows the engineers to design and optimize a multi-stage turbomachine within a much shorter time. The advantage of running circumferential average methods is more obvious as the number of blade rows is increased.

The unsteady pressure fluctuations on blade surfaces can be significant especially for modern high loading blade designs with smaller gaps between blade rows. As a result, other means to calculate the fluctuating pressures on the blades must be found in order to assure the design fatigue life. An approach using three-dimensional quasi-steady methodology was studied by Chen and Lee [1998]. It does provide pressure fluctuation data obtained from this method and is more econmomical than full unsteady analysis. However this can only be considered as an intermediate approach. The simulation of fully coupled unsteady rotor-stator interactions allows the total understanding of the flow physics. The three-dimensional fully coupled unsteady rotor-stator interaction simulation starts from Rai [1987] with an overlaid patched grid system. Other methods thereafter (e.g. Hah [1992]) more or less use the similar approach. Their calculations frequently modified the rotor and stator numbers to a simple arithmetic ratio like 2:3 or 1:1. The change of blade number was accompanied by a change of blade size in order to maintain its solidity or blockage. This however biased the physical problem. The predicted amplitude and frequency in the rotor-stator interaction are also biased. Moreover, these methods are very computational costly. As a result, they were mostly used in the final design verification or when a problem occurs. Erdos et al. [1977] proposed a phase-lagged method for unsteady analysis. This method uses only one blade pitch for each blade row. It

requires to store the unsteady flow data over an entire period so that the blades can feel periodical excitations from neighboring blade rows. The memory requirement is thus tremendous. This situation will become worse as the number of blade rows is large.

A simplified loosely coupled approach for unsteady turbomachinery flowfield predictions was investigated by Hodson [1985] and Ho and Lakshminarayana [1998]. They simply model the upstream unsteady disturbances with an incoming wakes. The wakes can be calculated separately from a steady state solution from an upstream blade row. Dorney et al. [1996] developed an iterated loosely coupled blade row method and applied it to a two-dimensional turbine stage. In their approach, the perturbations between two adjacent blade rows were iterated to updated values until convergence. It shows that the loosely coupled calculation can predict unsteadiness quite well but is an order of magnitude in computational efficiency compared with a fully couple unsteady analysis in a two-dimensional sense. Ho and Lakshminarayana's three-dimensional loosely coupled analysis modified the rotor/stator blade numbers from 42:40 to 40:40 so an equal pitch channel for stationary and rotating blade rows can be used. Blade size were scaled to maintain its blockage effect. Dorney et al. modified the stator/rotor numbers from 22:28 to 21:28 so an 3:4 blade ratios can be used to have a periodic boundary condition satisfied. Neither of the above loosely coupled method avoid the blade geometry modification.

The purpose of the present study is to develop a method that can solve a turbomachinery unsteady flowfield, but also has the following distinct advantages: Use only one blade channel for calculation while keeping the blade configuration unchanged. The numerical method used in the present study is a compressible viscous finite volume algorithm solving Reynolds averaged Navier-Stokes equations. The artificial dissipation terms similar to that used by Jameson is adopted to suppress the numerical oscillations. Four-stage Runge-Kutta scheme is used to advance the flow equations in time. Residual smoothing technique is employed to further accelerate convergence. Baldwin and Lomax algebraic turbulent model [1978] is used for the calculation of eddy viscosity. The UTRC large scale turbine test data were used to validate the CFD calculations.

2. NUMERICAL METHOD

The governing three-dimensional, compressible Navier-Stoke equations in integral form can be written as:

$$\frac{\partial}{\partial t}\int W\,dV+\oint F_c\cdot dA=\oint F_v\cdot dA+\int H\,dV \qquad (1)$$

where

$$F_c=E\vec{i}+F\vec{j}+G\vec{k}$$

$$F_v=R\vec{i}+S\vec{j}+T\vec{k}$$

and

$$W=\begin{bmatrix}\rho\\ \rho u\\ \rho v\\ \rho w\\ e\end{bmatrix}\quad E=\begin{bmatrix}\rho u'\\ \rho uu'+p\\ \rho vu'\\ \rho wu'\\ eu'+pu\end{bmatrix}\quad F=\begin{bmatrix}\rho v'\\ \rho uv'\\ \rho vv'+p\\ \rho wv'\\ ev'+pv\end{bmatrix}\quad G=\begin{bmatrix}\rho w'\\ \rho uw'\\ \rho vw'\\ \rho ww'+p\\ ew'+pw\end{bmatrix}$$

$$R=\begin{bmatrix}0\\ \tau_{xx}\\ \tau_{xy}\\ \tau_{xz}\\ \beta_x\end{bmatrix}\quad S=\begin{bmatrix}0\\ \tau_{yx}\\ \tau_{yy}\\ \tau_{yz}\\ \beta_y\end{bmatrix}\quad T=\begin{bmatrix}0\\ \tau_{zx}\\ \tau_{zy}\\ \tau_{zz}\\ \beta_z\end{bmatrix}\quad H=\Omega\begin{bmatrix}0\\ 0\\ \rho w\\ -\rho v\\ 0\end{bmatrix}$$

where e is the total energy per unit volume, $\vec{v}'=(u',v',w')$ is the relative velocity, its relationship with the absolute velocity $\vec{v}$ is:

$$\vec{v}'=\vec{v}-\vec{\Omega}\times\vec{r}$$

$$\vec{\Omega}=\Omega\vec{i}\ ,\ \vec{r}=(x,y,z)$$

The algebraic two-layer, eddy viscosity turbulence model derived by Baldwin and Lomax is used for the calculation of turbulent eddy viscosity.

The physical domain is divided into many small control volumes. The discretization form of eq. (1) is

$$\frac{d}{dt}(hw)+Q_c+Q_v=hH \qquad (2)$$

where h is the volume of grid, and

$$Q_c=\sum_k F_{ck}\cdot S_k$$

$$Q_v=\sum_k F_{vk}\cdot S_k$$

where k =1~6, S is the surface area on each side of control volume.

Equation (2) is solved using central differencing scheme which is second order accurate in space. In order to damp the numerical oscillation associated with central differencing scheme, artificial dissipation terms similar to that used by Jameson [1981] are considered. Eq. (2) can be written as:

$$\frac{d}{dt}(hw)+Q_c+Q_v-D=hH \qquad (3)$$

where D is the dissipative term:

$$D=(D_\xi+D_\eta+D_\zeta)w \qquad (4)$$

The $\xi-$ direction operator is given by:

$$D_\xi w=C_\xi(V_2 w_{\xi\xi}-V_4 w_{\xi\xi\xi\xi}) \qquad (5)$$

The terms V_2 and V_4 are given by

$$V_2=\mu_2\max(\nu_{i+1},\nu_i,\nu_{i-1})$$
$$V_4=\max(0,\mu_4-V_2) \qquad (6)$$

ν is expressed as

$$\nu_i=\frac{|p_{i+1}-2p_i+p_{i-1}|}{p_{i+1}+2p_i+p_{i-1}} \qquad (7)$$

The values of μ_2,μ_4 are chosen as 0.5 and 0.05 respectively. C is a coefficient that has an impact on the stability and accuracy of the solution. To minimize dissipation within viscous boundary layer, C_ξ is calculated from :

$$C_\xi=\frac{h}{\Delta t_\xi}\left(1+\frac{\Delta t_\xi}{\Delta t_\eta}+\frac{\Delta t_\xi}{\Delta t_\zeta}\right)\sigma \qquad (8)$$

whereσ=2/3□ Δt_ξ is the time step in the ξ-direction. It can be approximated as:

$$\Delta t_\xi=\frac{\Delta s_\xi}{V_\xi} \qquad (9)$$

Four-stage Runge-Kutta scheme is used to advance the flow equation (3) in time. To further accelerate convergence and allow larger time steps be used, implicit residual smoothing technique is used to minimize numerical instability. The residue R calculated above is smoothed after each Runge-Kutta stage by:

$$(1-\varepsilon_\xi\delta_{\xi\xi})(1-\varepsilon_\eta\delta_{\eta\eta})(1-\varepsilon_\zeta\delta_{\zeta\zeta})\overline{R}=R \qquad (10)$$

where $\delta_{\xi\xi},\delta_{\eta\eta},\delta_{\zeta\zeta}$ are standard second order differencing operator, and smoothing parameters $\varepsilon_\xi=\varepsilon_\eta=\varepsilon_\zeta=0.5$ are chosen .

The unsteady calculation starts from steady state solutions from a circumferential average calculation. In the circumferential average calculation, only one blade channel per blade row is used. The calculated exit condition of the stator form the inlet unsteady boundary condition for the downstream rotor blade row. On the other way around, the nonuniform inlet flow for the rotor calculated from circumferential average solution forms the stator unsteady condition at the exit. The unsteady interaction between the rotating and stationary blade rows are perturbed with respect to the mean values (the steady state solutions). The perturbed flow quantity at the stator exit can then be expressed as:

$$\hat{\phi}_s=(\phi_j-\bar{\phi})/\bar{\phi} \qquad (11)$$

where ϕ_j is the stator steady state solution (obtained from circumferential average calculation), $\bar{\phi}$ is the stator pitchwise mean value. The flow quantity at the rotor inlet would be the steady rotor value add the perturbation from the stator exit (equals rotor pitchwise mean multiplied by stator exit perturbation),

$$\phi_r=(\phi_j)_r+(\bar{\phi})_r\cdot\hat{\phi}_s \qquad (12)\,.$$

Similarily, the flow quantity at the stator exit can be expressed as the steady stator exit value plus the pertubation from the rotor inlet,

$$\phi_S = (\phi_j)_S + (\bar{\phi})_S \cdot \hat{\phi}_r \qquad (13)$$

Since only pitch per blade row is used, and the blade numbers are different, the perturbation period felt by the rotor is different from that felt by the stator. Thus, one must keep the flow data of the neighboring flow channels in memory. Although the unsteady flow quantity calculated from eqs (12) and (13) are not periodical from blade to blade, and also are varied from time to time, the steady state solutions for the two blade rows are unchanged within one blade passing period. It must be emphasized that the initial steady state solutions are obtained from circumferential average calculations. The steady state solutions are updated by a time average method after every blade passing period is completed. The iteration process is continued until a converged solution is achieved.

3. BOUNDARY CONDITIONS

The boundary conditions for turbomachinery inlet, exit, solid surface, periodic boundaries and at mixing planes are discussed below.

One-dimensional Riemann Invariant non-reflection boundary condition is adopted at the inlet boundary. At the exit boundary, the pressure at mid-span is prescribed. Radial equilibrium equation is used to calculate the pressures along the exit plane from hub to tip. At the solid surfaces, both non-slip boundary condition and non-penetration condition are considered. That is to force the relative contravariant velocities on the wall surface to be zero. Periodic boundary condition is imposed on the blade-to-blade upstream of the leading edge and downstream of the trailing edge for each blade row to ensure a correct converged solution. This is to average the extrapolated lower boundary (at j=1) and the extrapolated upper boundary (at j=jmax) values.

For circumferential average calculation, the treatment at the mixing plane is an important step. The mixing planes are located approximately midway between two adjacent blade rows. The mixing planes for circumferential average calculations are treated as interior points rather than ordinary inlet or exit boundary points. The present mixing plane treatment is similar to that of Chen [1996] and Denton [1992]. The variables at one side of mixing plane are first extrapolated to obtain the values at mixing plane and then circumferentially area averaged.

$$\phi^s_{ave} = \sum_{j=1}^{j=j\max} (\phi^s_j) A^s_j \Big/ \left(\sum_{j=1}^{j=j\max} A^s_j \right) \qquad (14)$$

$$\phi^r_{ave} = \sum_{j=1}^{j=j\max} (\phi^r_j) A^r_j \Big/ \left(\sum_{j=1}^{j=j\max} A^r_j \right) \qquad (15)$$

The superscripts s and r denote stator and rotor respectively. The new circumferential average values at the mixing plane are the simple arithmetic mean of the two circumferentially averaged values from two sides.

$$\phi_{ave} = (\phi^s_{ave} + \phi^r_{ave})/2 \qquad (16)$$

The variables at either side of the mixing plane are adjusted proportionally to the ratio between the new and old circumferential values.

$$\phi^s_{new} = \phi^s_{old} \cdot \frac{\phi_{ave}}{\phi^s_{ave}} \qquad (17)$$

$$\phi^r_{new} = \phi^r_{old} \cdot \frac{\phi_{ave}}{\phi^r_{ave}} \qquad (18)$$

These values are then considered as the new boundary values at the mixing planes for the next step calculation. This mixing plane modeling results in circumferentially nonuniform flow properties at the mixing planes.

Since unequal pitch channels are used, there is no unsteady periodic boundary condition as that in a steady state sense. The unsteady values at the steady periodic lines are simply extrapolated from interior points at each time step.

4. RESULTS AND DISCUSSIONS

The UTRC Large Scale Turbine is used here as the baseline configuration. Its geometrical parameters are shown in Table 1. In the present study, only the first stator and rotor are considered. The gap between stator and rotor is 15% stator chord.

Table 1 UTRC 1 1/2 Stage Large Scale Turbine

	1st stator	1st rotor	2nd stator
blade number	22	28	22
chord (m)	0.151	0.161	0.164
hub radius (m)	0.610	0.610	0.610
tip radius (m)	0.762	0.762	0.762

The grid system for the turbine is generated using the interactive grid generation procedure developed by Lee et al. [1995]. The grid system is the same as that used in a previous study [Chen and Lee (1998)]. A two-dimensional view of the the grid system for the 1.5 stage turbine is shown in fig. 1. The grid system has 89x33x25 grids for the first stator, 85x33x25 grids for the rotor, and 99x33x25 grids for the second stator. The total number of grids is 225,225. For the present study, only the stator and rotor grids are considered. Good orthogonality, smoothness and clusterness are achieved.

The circumferential average solution is used as the initial condition for unsteady calculations. Fig. 2 shows the circumferential average solution for the stator from near the hub to near near the tip. The results compared well with the data [Dring et al. (1982)]. Fig. 3 shows the circumferential average solution for the rotor. Some uncertainty in the data for the rotor is shown in the figure. Again the agreement is good. Fig. 4 is the pressure distributions at various time steps for the stator and rotor at midspan. The circles in the figure are the time average results over one blade passing period. The time average results become the new steady state solution. The final converged steady state solutions at several blade heights are shown in figs. 2 and 3. The solutions for both the initial circumferential average solution and the final time averaged steady state solutions are similar although some discrepancies are found near the hub and the tip.

The pressures at 6 locations (3 near stator exit and 3 near rotor inlet shown in fig. 5) are monitored to make sure the unsteady pressures do reach periodical solutions. (Note that the figure is plotted of equal pitch used in the other calculations) Fig. 6 shows the unsteady pressures at these 6 monitor points. It can be seen that the unsteady pressures reach near periodical condition very quickly after only one blade passing period.

The stator exit velocities at the midspan mixing plane boundary are shown in fig. 7 for one rotor blade passing period. The stator wake at pitch=0.9 has some significant velocity fluctuation due to interaction with the downstream rotor. The global wave moves from pitch=1 to pitch=0 due to rotor motion. The time average velocity at stator exit mixing plane is shown in fig. 8. It should be pointed out that the calculated result has been shifted tangentially in order to compare against the original measurement data. Although the predicted wake velocity deficit is larger, the overall trend agrees quite well with data. Fig. 9 is the rotor inlet velocities at the mixing plane boundary. Global perturbation wave motion is moving in opposite direction relative to that in the stator. The stator viscous wake influence on the rotor is obvious as it moves with with the global wave. The results show that the rotor influence on the the upstream stator is basically a potential effect. And, the stator influence on the rotor both the potential and viscous wake effects are important. The time average velocity at rotor inlet mixing plane is shown in fig. 10. The fluctuation is larger than that due to the stator wake (fig. 8).

The pressure fluctuation amplitudes for the unsteady calculations are shown in fig. 11. The predictions agreed quite well with the data especially the maximum amplitude and trend at the critical areas (trailing edge of stator and leading edge of rotor), although some overprediction on the suction surface of stator and underprediction on the suction surface of rotor.

The analysis shows that a three-dimensional unsteady analysis using single unequal pitch for a turbine stage can be successful if the interactions between the stationary and rotating blade rows are properly modeled. The biggest advantage of using this approach is computational efficiency and maintain the blade configuration intact. Thus, the predicted flowfield could be more realistic. The computations were performed on a DEC-8400 machine. Roughly 1500 time steps per stator passing period, and 3 subiterations per time steps were used. One entire unsteady calculation (including initial circumferential average calculation) of about 10 stator passing periods (or roughly 13 rotor passing periods) took about 6 days in CPU.

5. CONCLUSIONS

A loosely coupled blade row analysis method is used on a three-dimensional single stage turbine unsteady analysis. Unlike the other loosely coupled or fully coupled methods, the present approach uses only one blade pitch for each blade row while the blade configuration is unmodified. Circumferential average analysis result using the same computational domain

is used as the initial condition for unsteady analysis. The use of circumferential average solution as the starting point makes the predicted unsteady periodical solution can nearly be achieved after only one blade passing period. The steady state solution is a time average result over a complete blade passing period. Basically both steady state solution and circumferential average solution agree well with measured data, although some differences exist between the two solutions. The predicted unsteady solutions show thw that the unsteady interaction between two adjacent blade rows can be reasonably well simulated. It is clear that the influence from the downstream blade row basically is due to a potential effect and the influence from the upstream blade row is due both to viscous wake and potential effects. Despite the present approach is considered as an approximate solution compared with a fully coupled unsteady calculation, the result is very encouraging.

6. ACKNOWLEDGEMENT

The present study is supported by the National Science Council (NSC) of the Republic of China under the contract number NSC87-0210-D-006-003.

7. REFERENCES

1. Adamczyk, J.J.,Celestina,M.L.,Beach,T.A.and Barnett, M."Simulation of Three-Dimensional Viscous Flow within a Multistage Turbine" ASME J.of Turbomachinery, Vol 112,p370-376, 1990

2. Baldwin, B.S. and Lomax, H., "Thin Layer Approximation and Algebraic Model for Separation Turbulent Flows" AIAA 16th Aerospace Sciences Meeting 1978, 78-257.

3. Chen, S. H., "The Flow Analysis of A Three-Dimensional Multistage Turbomachinery Blade Design", Proceedings of the 6th International Symposium on Transport Phenomena and Dynamics of Rotating Machinery, Vol. 2, 1996, pp.277-286.

4. Chen, S. H. and Lee, L. C., "Three-Dimensional Multi-Blade-Row Turbomachinery Flow Analysis," 7th ISROMAC, February 1998.

5. Dawes, W.N., "Toward Improved Through-flow Capability: the use of Three-Dimensional Viscous Flow Solvers in a Multistage Enviroment" J. of Turbomachinery, Vol 114 p8-17, January, 1992.

6. Denton, J.D., "The Calculation of Three-Dimensional Viscous Flow Through Multistage Turbomachines" J. of Turbomachinery, Vol 114 pp18-26, January, 1992.

7. Dorney, D. J., Davis, R. L. and Sharma, O. P., "Unsteady Multistage Analysis Using a Loosely Couple Blade Row Approach," J. of Propulsion and Power, Vol. 12, No. 2, March 1996.

8. Dring, R. P., Joslyn, H. P., Hardin, L. W., and Wagner, J. H., "Turbine Rotor-Stator Interaction", J. of Engineering for Power, Vol. 104, No. 10., 1982, pp.729-742.

9. Dring, R. P., Blair, M. F., Joslyn, H. D., Power, G. D., and Verdon, J. M., "The Effects of Inlet Turbulent and Rotor/Stator Interactions on the Aerodynamics and Heat Transfer of a Large-Scale Rotating Turbine Model", Part I, Final Report, NASA Contract Report CR4079, May 1986.

10. Dring, R. P., Joslyn, H. D., Blair, M. F., "The Effects of Inlet Turbulent and Rotor/Stator Interactions on the Aerodynamics and Heat Transfer of a Large-Scale Rotating Turbine Model", Part IV, Aerodynamic Data Tabulation, NASA Contract Report CR179496, May 1988.

11. Erdos, J. I., Alzner, E. and McNally, W., "Numerical Solution of Periodic Transonic Flow Through a Fan Stage," AIAA Journal, Vol. 15, No. 11, pp.1559~1568, 1977.

12. Hah, C., "Navier-Stokes Analysis of Three-Dimensional Unsteady Flows inside Turbine Stages", AIAA paper no. 92-3211, 28th Joint Propulsion Conference, July 1992.

13. Ho, Y. H. and Lakshminarayana, B., "A Loosely Coupled Unsteady Flow Simulation of a Single Stage Compressor", IJCFD, Vol. 10, 1998, pp.73-89.

14. Hodson, H. P., "An Inviscid Blade-to-Blade Prediction of Wake-Generated Unsteady Flow", Journal of Engineering for Gas Turbines and Power, Vol. 107, April 1985, pp.337-344.

15. Jameson, A., Schmidt, W., and Turkel, E., "Numerical Solutions of the Euler Equations by Finite Volume Methods Using Runge-Kutta Time-Stepping Schemes", AIAA paper 81-1259, June 1981.

16. Lee, L. C., Chen, S. H., Shu, S. B., and Hsu, W. Y., "Interactive Grid Generation for Turbomachinery Applications", The Chinese Third CFD Conference, August 1995.

17. Ni, R.H. and Bogoian, J.C., "Prediction of 3D Multistage Turbine Flow Field Using a Multiple Grid Euler Solver" AIAA paper no. 89-0203, January 1989.

18. Rai, M.M., "Unsteady Three-Dimesnioal Navier-Stokes Simulations of Turbine Rotor-Stator Interacton" AIAA-87-2058,1987.

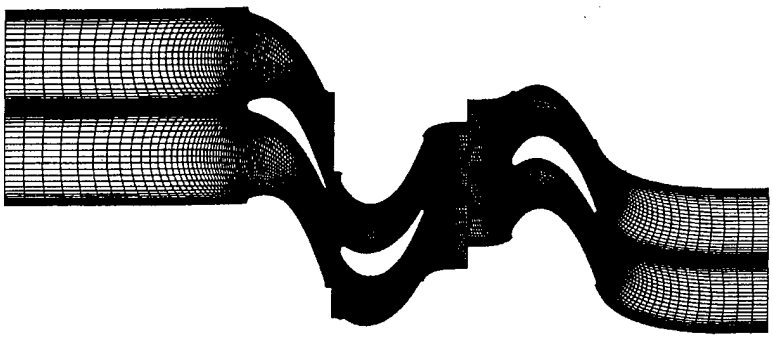

Fig. 1 Grid system for UTRC turbine calculation.

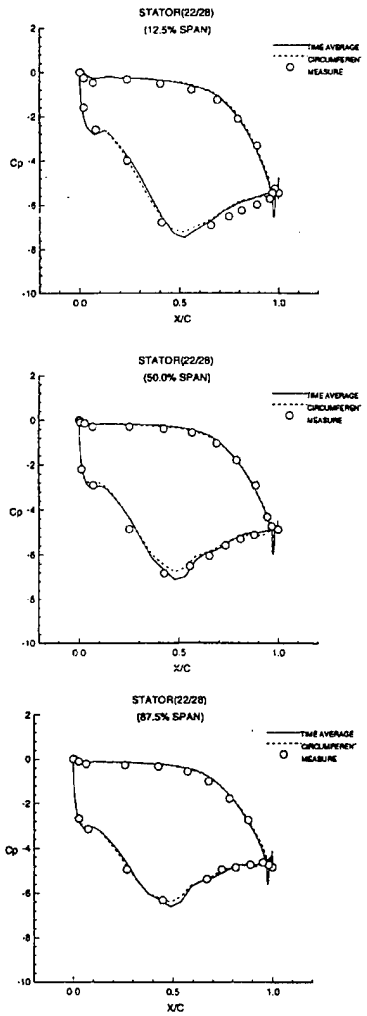

Fig. 2 Circumferential average and time average solutions for stator.

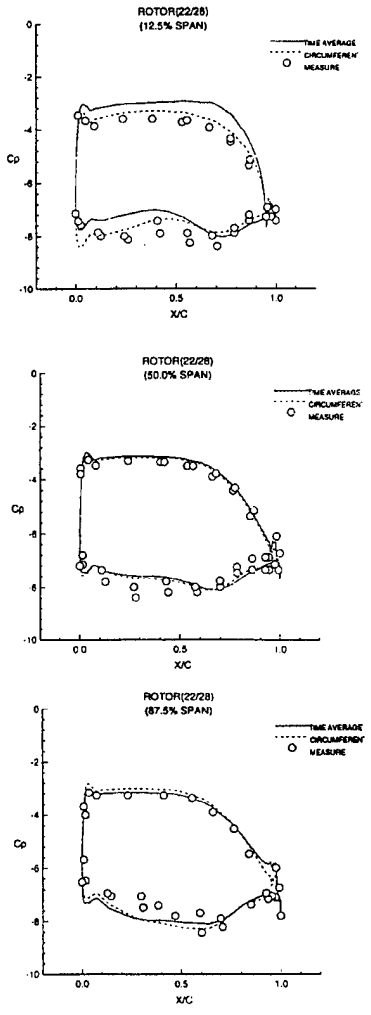

Fig. 3 Circumferential average and time average solutions for rotor.

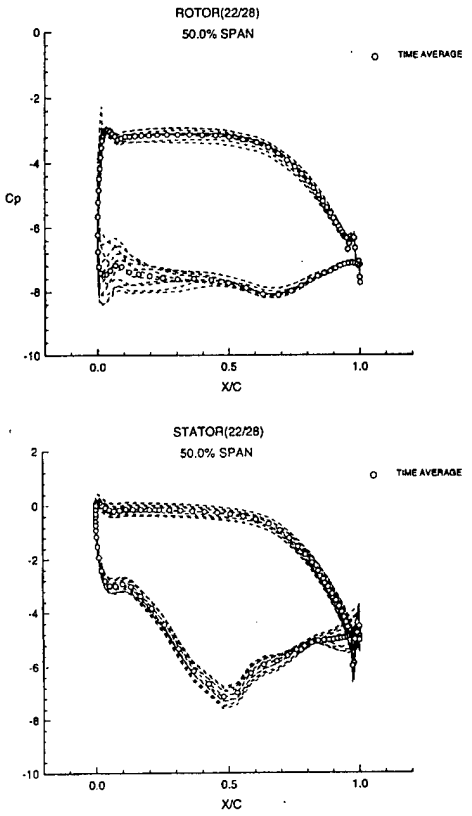

Fig. 4 Midspan pressure distributions for stator and rotor at different time steps.

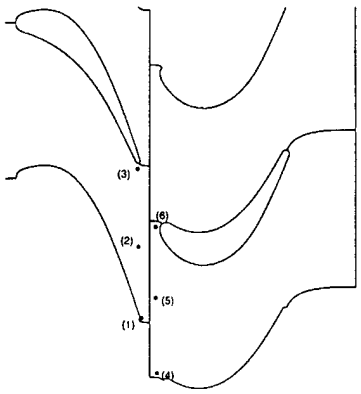

Fig. 5 Monitor point locations.

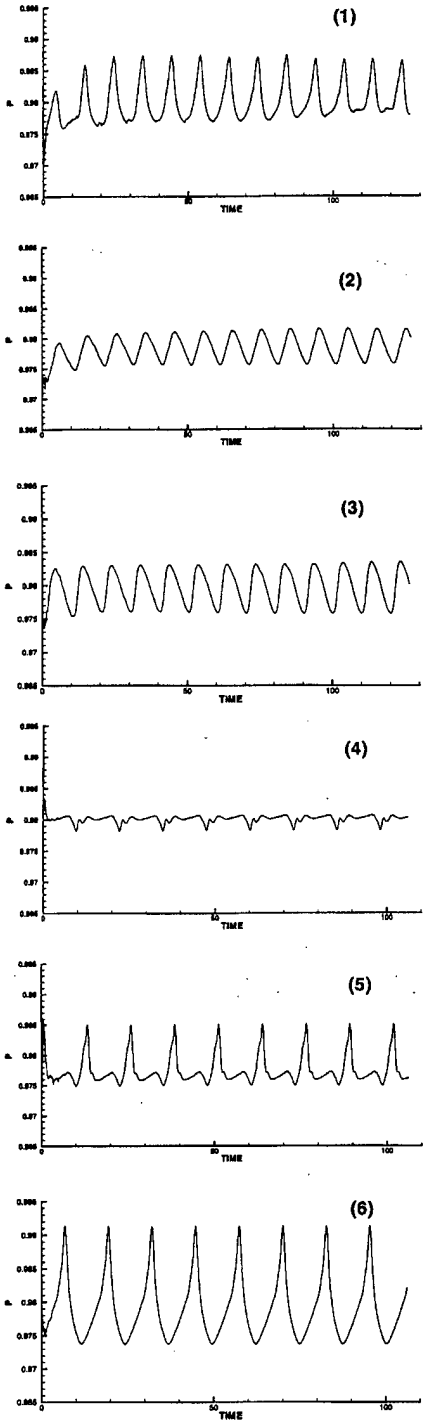

Fig. 6 Pressure variations at 6 monitor points.

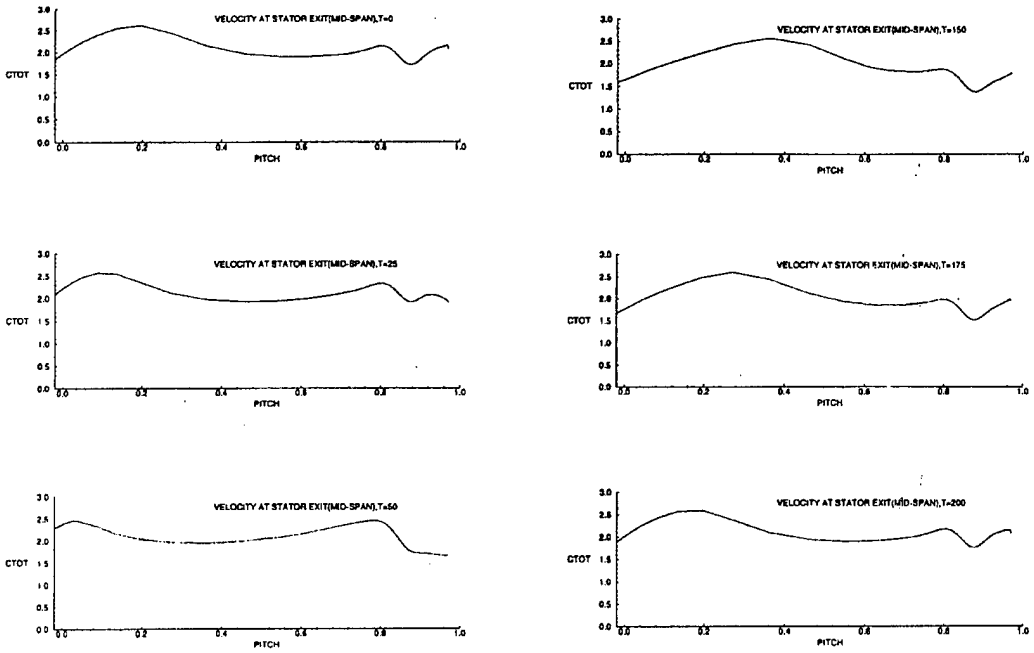

Fig. 7 Unsteady velocity at stator exit.

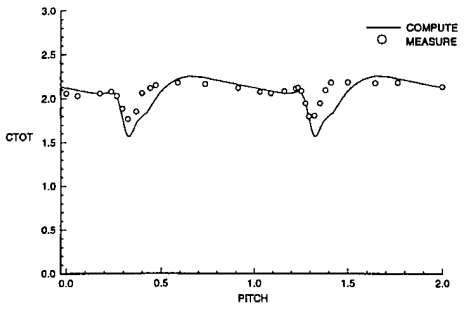

Fig. 8 Time average velocity at stator exit.

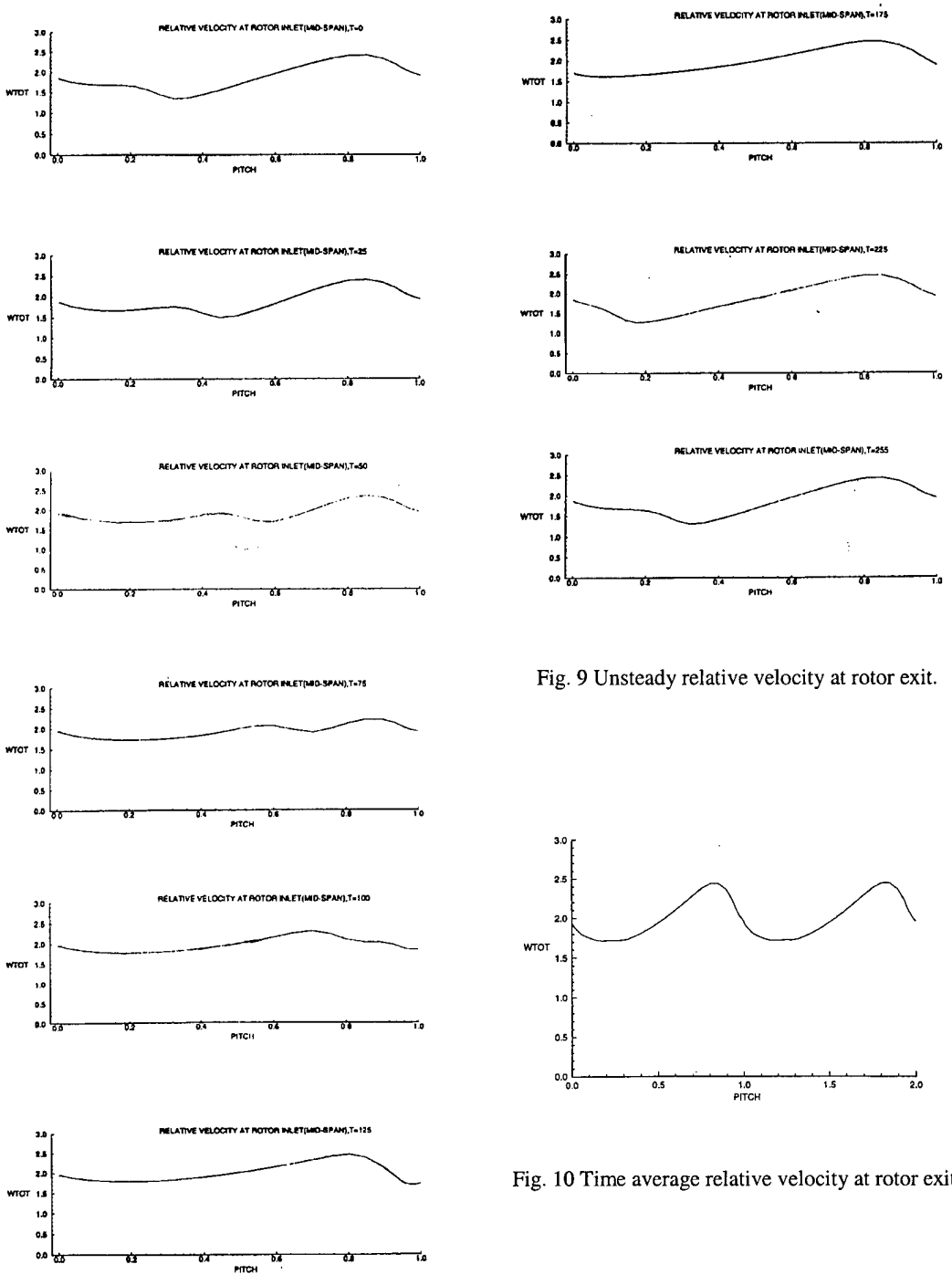

Fig. 9 Unsteady relative velocity at rotor exit.

Fig. 10 Time average relative velocity at rotor exit.

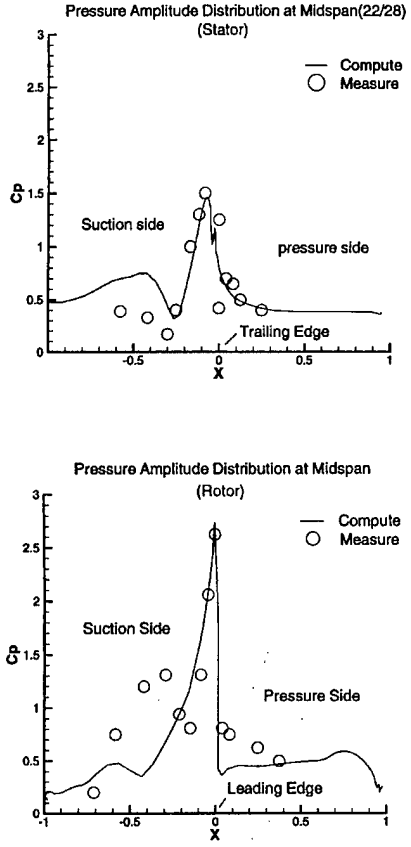

Fig. 11 Unsteady pressure fluctuation amplitudes.

Back